[1)]Of course, SNS of the indicated type—excited by constant external forces—do not exhaust all the diversity of SNS, and the Markov FDR derived below have a more limited circle of applications than the initial relations. We shall not touch upon cases in which the constant forces do not destroy the equilibrium but the SNS can arise under the action of periodic forces (resonantly interacting with the system). Moreover, an SNS can occur even in the absence of dynamic perturbations as a result of nonequilibrium boundary conditions (thermal perturbations). True, in this case one can sometimes replace the nonequilibrium conditions by certain effective forces and use dynamical FDR.

[2)]As in Ref. 1, we use a scalar notation for vectors and tensors; only in case of necessity do we transform to the full description.

[3)]The term "macrovariable" can apply also to an individual particle (or an ensemble of noninteracting particles).

[4)]These relations yield a generalization of the Kubo formula to the nonlinear case.

[5)]It is clear that the coefficients Γ' take into account the nondissipative contribution of the thermostat to the motion of the macrovariables, for example, the renormalization of their eigenfrequencies as a result of the interaction with the thermostat. The same can also be said about the Markov kinetic coefficients K_1' introduced below.

[6)]This is certainly true for a linear system.

[7)]We note that formulas (11)-(13) confirm certain results of the phenomenological approach,[6] in which the condition of the maximum of informational entropy for a given value of dissipation (or, in our terminology, at given mean values of the currents) is used to construct the distribution functions in the SNS.

[8)]As before, we use the real variable u instead of $\dot{u}$, since we are interested only in the formal structure of the relations.

[1]G. N. Bochkov and Yu. E. Kuzovlev, Zh. Eksp. Teor. Fiz. 72, 238 (1977) [Sov. Phys. JETP 45, 125 (1977)].

[2]R. L. Stratonovich, Vestnik, MGU, fiz. astr., 5, 16 (1962).

[3]R. L. Stratonovich, Vestnik, *ibid.* 4, 84 (1967).

[4]R. L. Stratonovich, Izv. Vuzov, Radiofizika 13, 1512 (1970).

[5]A. N. Malakhov, Kumulyantnyĭ analiz sluchaĭnykh negaussovykh protsessov i ikh preobrazovaniĭ (Cumulant Analysis of Random Non-Gaussian Processes and Their Transformations) Sovetskoe radio 1978.

[6]H. Sato, Prog. Theor. Phys. 57, 1115 (1977).

[7]W. Feller, Introduction to Probability Theory and Its Applications, Vol. 2, Wiley, 1971.

[8]K. Seeger, Semiconductor Physics, Springer, 1974.

[9]A. Van der Ziel, Noise, Prentice-Hall, 1970.

Translated by R. T. Beyer

Two-dimensional electronic phenomena in germanium bicrystals at helium temperatures

B. M. Vul and É. I. Zavaritskaya

P. N. Lebedev Physics Institute, USSR Academy of Sciences

(Submitted 30 August 1978)
Zh. Eksp. Teor. Fiz. **76**, 1089–1099 (March 1979)

The two-dimensional conductivity, Hall effect, and Shubnikov–de Haas oscillations on the intergrowth surfaces of germanium bicrystals with inclination angles $6° \leq \theta \leq 30°$ were investigated at helium temperatures in magnetic fields up to 150 kOe. A transition from metallic to thermally activated conductivity was observed at an angle $\theta \approx (8–9)°$. The minimal metallic conductivity is found to be $\sigma_{min} \approx e^2/2\pi\hbar$, in agreement with the simplest theoretical estimates. Shubnikov–de Haas oscillations are observed in the metallic conductivity region at $\theta \gtrsim 20°$. They are shown to be due to the contribution of the light holes. It is established that the conductivity decreases sharply with decreasing angle θ, owing to onset of one-dimensional conduction conditions. The anisotropy of the conductivity is investigated. A model is proposed to explain the observed phenomena.

PACS numbers: 72.20.Ht, 72.15.Gd

Interest in the so-called one-dimensional and two-dimensional systems has increased of late in connection with searches for high-temperature superconductivity and superfluidity. Electronic phenomena in systems that are close to two-dimensional were investigated in inversion layers of silicon in metal-insulator-semiconductor structures. In these structures it is easy to control the carrier density by an external field, but it is difficult to obtain identical oxide layers, and this introduces an uncertainty in the interpretation of the obtained data that characterize a two-dimensional system.[1] A more reliable model of a two-dimensional system, in our opinion, consists of highly conducting layers adjacent to the cleavage planes of germanium crystals. They are formed at a junction of single crystals and are characterized by a sufficiently well ordered structure, as confirmed by the small scatter of the carrier densities and mobilities in these layers, as obtained in various laboratories of the world.[2,3]

1. PREPARATION OF BICRYSTALS

The germanium bicrystals were grown by the Czochralski method on a double seed crystal by a method similar to that described in Ref. 2. The double seed was prepared by cutting a single-crystal ingot into two at a specified inclination angle $\theta/2$ to the [100] axis,

0038-5646/79/030551-07$02.40

followed by turning one half of the crystal relative to the other and joining the two together. Edge dislocations are then produced in the intergrowth plane, along the turn axis, with an average distance between dislocations[2]

$$d=b/2\sin(\theta/2), \qquad (1)$$

where b is the Burgers vector, approximately equal to the lattice constant a. In germanium $a\approx 5$ Å.

X-ray investigations have shown that in our samples some parts of the crystal, besides being turned through the specified angle θ, made also small angles with the other axes. However, since the inclination angle θ was significantly larger than the other angles, we used in the analysis of the measurements results a simplified model of the dislocation tubes, and determined the number of dislocations in accord with (1).

2. ELECTRIC CONDUCTIVITY

A large part of the measurements was made on samples in the form of a parallelepiped cut from the ingot in such a way that the current was either parallel or perpendicular to the dislocation tubes. The initial crystals were in most cases of n type with resistivity from 1 to 40 Ω-cm and with angle θ from 6 to 30°. The contacts produced by fusing-in indium were located as shown in Fig. 1. The usual sample dimensions were $L=10$ mm, $s=4-5$ mm and $h=2-3$ mm. The contacts were ohmic for p-Ge and rectifying for n-Ge.

For the n-Ge bicrystals with angles $10°<\theta<30°$ it was easy to separate the conductivity of the layer adjacent to the cleavage plane from the total sample conductivity. As seen from Fig. 2, the results of the measurement of the bicrystals in this case pertain in practice to this high-conducting layer up to temperatures $T\lesssim 30$ K. For bicrystals with the same angles, but made of p-Ge doped with copper, the electric conductivity of the main crystal could shunt the conductivity of the layer adjacent to the cleavage plane only at $T>20$ K, as seen from the data also shown in Fig. 2.

With decreasing θ, the separation of the layer conductivity from the total sample conductivity in bicrystals with angle $\theta<10°$ became progressively more difficult, because of the lifting of the degeneracy of the carriers in the layer. The data on the electric conductivity of the layer for these samples are reliable only at temperatures $T<7$ K, when the conductivity of the initial crystal can be neglected.

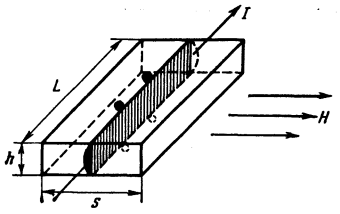

FIG. 1. Shape of samples and their contacts. The intergrowth plane is shaded.

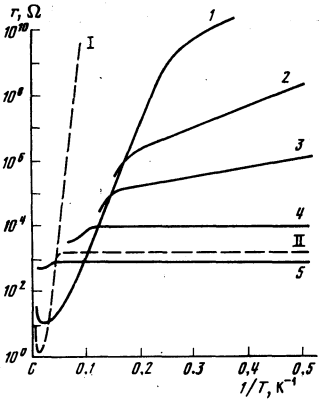

FIG. 2. Temperature dependence of the resistance of bicrystals. The solid and dashed lines pertain to n-Ge and p-Ge, respectively. Curves I and 1—single crystals, 2, 3, 4, 5, and II—bicrystals with angles θ equal to 7, 8.5, 10, 25, and 27° respectively.

The results of the low-temperature measurement of the resistance of samples with angle $7°\lesssim\theta\lesssim 30°$ are shown in Figs. 3 and 4 for current directed along ($\rho_\parallel$) and across ($\rho_\perp$) the dislocation axis, respectively. In these figures $\rho=rh/L$, where r is the measured resistance, which in all cases is less than the resistance of the corresponding single crystal. As seen from the data, the plots of $\rho(1/T)$ form two families of curves. The resistance of the samples with angle $\theta<10°$ increases exponentially with decreasing T, whereas that of the samples with $\theta>10°$, while not the same for the different samples, is independent of temperature, a typical feature of degenerate semiconductors.

The maximum resitance of degenerate samples that is still independent of temperature is the same for current flowing parallel and perpendicular to the dislocations, and is equal to

$$\rho_0\approx 25\ \text{k}\Omega_\square.$$

This can be explained by starting from the premise that the conducting part of the crystal, adjacent to the cleavage plane, is so thin that its electric conductivity can be treated as in a two-dimensional medium.[4] In this case the carriers density in the degenerate electron gas is

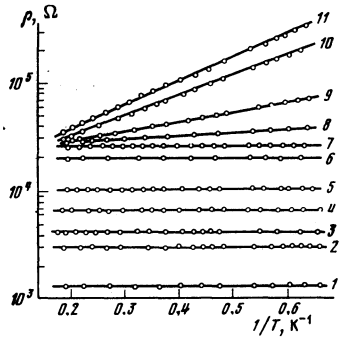

FIG. 3. Temperature dependence of $\rho_\parallel$ in bicrystals with different angles θ: $1-\theta\sim 28°$, $2-\theta\sim 20°$, $3-\theta\sim 16°$, $4-\theta\sim 12°$, $5-\theta\sim 10°$, $6-\theta\sim 9°$, $7-11-\theta=8-7$.

$$n=P^3/2\pi\hbar^3, \quad (2)$$

where P is the electron momentum on the Fermi level, and the conductivity is

$$\sigma=ne\mu=(e^2/2\pi\hbar^2)Pl, \quad (3)$$

where $\mu=el/mv=el/P$ is the mobility, l is the mean free path, v is the carrier velocity, and e is the electron charge. Using the uncertainty relation

$$Pl\geqslant\hbar, \quad (4)$$

we find that $\sigma_{min}\approx e^2/2\pi\hbar\approx 4\cdot 10^{-5}\ \Omega^{-1}$, which agrees with our value of ρ_0.

The resistance of samples with $\rho>\rho_0$ is $\rho\sim\exp(\varepsilon_a/kT)$, if we introduce the activation energy ε_a. A plot of the latter against the resistance, for samples with different ρ, takes the form shown in Fig. 5. It follows from these data that the activation energy sets in at $\rho_0\approx 25$ kΩ and at first increases steeply with increasing ρ. Obviously the carrier degeneracy is not immediately lifted with increasing distance between dislocations, and the average carrier energy is then determined both by the temperature and by the position of the Fermi level. When the degeneracy is lifted, the average energy and hence the carrier mobility is determined to an ever greater degree by the temperature, and consequently the conductivity will vary noticeably with temperature. We have observed a similar phenomenon in a study of the electric conductivity of compensated gallium arsenide in strong magnetic fields.[5]

The electric conductivity of the germanium bicrystals is isotropic only at inclination angles $\theta=25°-30°$. At smaller angles the conductivity is anisotropic. Figure 6 shows the dependence of the electric conductivity parallel ($\sigma_\parallel$) and perpendicular ($\sigma_\perp$) to the dislocations on the distance between the dislocation axes. The data of Fig. 6 pertain to the batter samples, having the highest conductivity at the given angle ($\theta<20°$). As seen from these data, in the region 10 Å $<d<$ 30 Å the conductivity $\sigma_\parallel$ remains practically constant, whereas $\sigma_\perp$ decreases monotonically with increasing d.

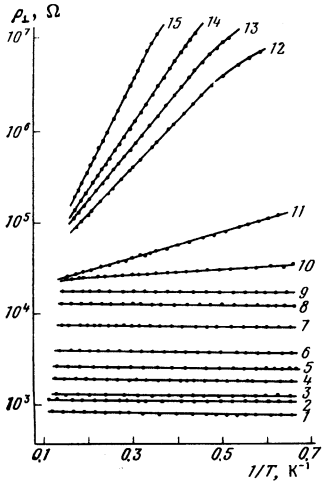

FIG. 4. Temperature dependences of $\rho_\perp$ in bicrystals: 1–3 – $\theta\sim 28°$; 4, 5 – $\theta\sim 20°$, 6 – $\theta\sim 16°$, 7 – $\theta\sim 12°$, 8, 9 – $\theta\sim 10°$, 10 – 15 – $\theta=(8.5–7.0)°$.

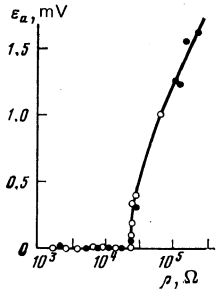

FIG. 5. Dependence of activation energy ε_a on the resistance at $T=6K$, ●—for $\rho_\perp$, ○—for $\rho_\parallel$.

At $d>30$ Å both $\sigma_\parallel$ and $\sigma_\perp$ decrease strongly, by about two or three orders of magnitude when d is decreased by only 10 Å. The relative decrease of the electric conductivity, characterized by the anisotropy coefficient $\alpha=\sigma_\parallel/\sigma_\perp$, goes through a maximum at $d\approx 35–40$ Å. The same anisotropy results were obtained also with samples having a special geometry by Montgomery's method.[6] These samples were cubes 3×3×3 mm with the intergrowth plane in the middle. The contacts were small spheres of indium soldered to the four corners of this plane.

3. HALL EFFECT

The measurements were performed, in weak fields $H\leqslant 5$ kOe with an electromagnet and in strong magnetic fields up to 150 kOe with a Bitter-type solenoid, by the usual procedure, with both the current direction and the magnetic field varied. A linear dependence of the Hall voltage with current was observed in all the measurements.

Measurements made in the range $1.6\leqslant T\leqslant 10$ K on the samples with resistance $\rho<\rho_0$ have shown that the Hall emf, and hence the carrier density, does not depend on the temperature. The sign of the Hall emf corresponded to p-type conductivity for all samples. In most samples the hole density calculated from the elementary relation

$$n=1/Re, \quad R=V_H/iH \quad (5)$$

(V_H is the voltage on the Hall contacts) turned out to be approximately the same and equal to $n=(4.5-6)\times 10^{12}$ cm^{-2}. For only one group of samples, with angle $\theta\approx 28°$, which were stored for several years, did the hole density determined in this manner turn out to be 2–4 times larger. These samples were subsequently used to measure the Shubnikov–de Haas effect.

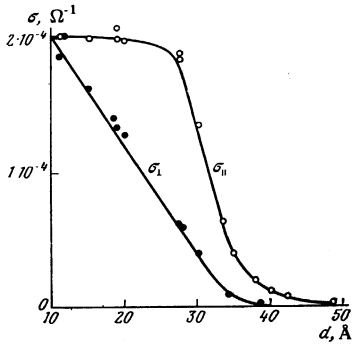

FIG. 6. Dependences of the electric conductivities $\sigma_\parallel$ and $\sigma_\perp$ on the distance d between dislocations ($T=4.2$ K).

It is known that if no account is taken of the spin-orbit interaction, the valance band of germanium, includes bands of light and heavy holes. In a perfect crystal the effective masses of the heavy and light holes are $m_h \approx 0.36 m_0$ and $m_l = 0.042\ m_0$, respectively.[7] In the presence of carriers of both types and of like sign, the Hall coefficient is equal to

$$R_{H\to 0} = \frac{r}{e}\frac{n_l\mu_l^2 + n_h\mu_h^2}{(n_l\mu_l + n_h\mu_h)^2}, \tag{6}$$

where the subscripts l and h pertain to the light and heavy holes, respectively, and r is the Hall factor. In the conducting layer of a germanium bicrystal, at low temperatures, the scattering is predominantly by charged centers with concentration $N_i \approx 10^{13}$ cm^{-2}. Since the light and heavy holes have the same energy and are scattered by the same centers, it follows[8] that $\tau_l/\tau_h \approx v_h/v_l$ and

$$\mu_l/\mu_h \approx (m_h/m_l)^{1/2}. \tag{7}$$

In the two-dimensional case under degeneracy, the carrier density is $n = mE_F/\hbar^2$, where E_F is the Fermi energy; the density ratio is therefore

$$n_l/n_h = m_l/m_h. \tag{8}$$

Using (7) and (8), we get from (6)

$$R_{H\to 0} \approx 1.1r/n_h. \tag{9}$$

In the calculation of the hole density, recognizing that the electron gas is degenerate as well as that the scattering is by the charged centers and at low temperatures, we can assume a Hall factor $r \approx 1$ (Ref. 1) and a heavy-hole density $n_h \approx 1/Re$. Analysis of the three-dimensional problem leads to a similar conclusion.

Measurement have shown R to be independent of the magnetic field intensity up to $H \leq 40$ kOe. This also confirms that $r \approx 1$. In magnetic fields $40 < H < 150$ kOe Hall-effect oscillations were observed with the same period as the magnetoresistance oscillations in these samples. They are due, as shown in Ref. 10, to the contribution of the oscillating magnetoresistance component to the magnetostriction.

4. CARRIER MOBILITY

In the overwhelming majority of the degenerate samples with inclination angle $8 \leq \theta \leq 30°$, with the exception of some samples that were stored for a long time, the carrier density was practically the same, and the carrier mobility differed by an approximate factor of 6—from 300 to 50 cm^3/V-sec. The smallest value $\mu \approx 50$ cm^2/V-sec corresponds to the minimum of the metallic conductivity, when $Pl \approx \hbar$, where P is the carrier momentum and l is the mean free path. Since the carrier density is $n = \frac{1}{2}\pi^{-1}(P/\hbar)^2$, the corresponding mean free path at $n \approx 5 \times 10^{12}$ cm^{-2} is $l \sim 20$ Å.

Since the carrier mobility in samples with metallic conductivity and equal carrier density exceeds its minimum value by as much as six times, the mean free path in them can obviously reach $l \sim 120$ Å, greatly exceeding the effective thickness of the conducting layer. The observed relatively large mobilities in the surface layer confirm that the transport phenomena in these layers can be regarded in our case as taking place in a two-dimensional medium, and the effects due to the layer thickness can be neglected.

The dependence of the mobility on the distance d between the dislocations is shown in Fig. 7. It is seen that the mobility remains almost constant when the carriers move along the dislocations, when the distance between them changes from 10 to 30 Å. Obviously, at these distances the hole density is quite uniformly distributed along the dislocations.

At $d > 30$ Å the mobility decreases sharply, owing to the transition from metallic to activation conductivity. With increasing d, obviously, potential barriers between the dislocations axes appear and grow as a result of the concentration of the holes near them.

5. SHUBNIKOV–de HAAS OSCILLATIONS

Unlike the Hall effect, which is determined by the concentration of the heavy holes, the predominant role in the Shubnikov–de Haas oscillations is played by the light holes. In fact, the distance between the Landau levels is inversely proportional to the carrier mass, so that it can turn out to be larger than the level smearing in the case of the light holes.

Measurements of the resistance and of the Hall coefficients have shown that at $H > 50$ kOe the functions $\rho(H)$ and $R(H)$ reveal oscillations whose amplitudes increase with the magnetic field intensity and reach approximately 2% at $H = 100$ kOe, whereas the total change of $\Delta\rho/\rho_0$ and $\Delta R/R_0$ in the field range $0 < H < 150$ kOe is ~10%.

It is known that the period of the Shubnikov–de Haas oscillations is

$$\Delta(1/H) = e\hbar/mcE_F, \tag{10}$$

where E_F is the Fermi energy at $H = 0$, m is the effective carrier mass. In the two-dimensional isotropic case and at a quadratic disperion law we have $E_F = \pi\hbar^2 n/m$ and the period is

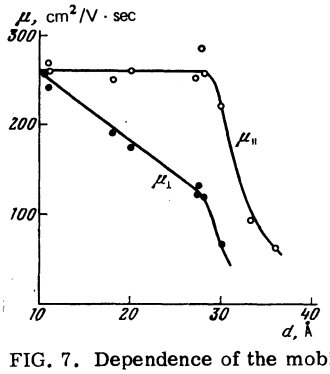

FIG. 7. Dependence of the mobilities $\mu_\parallel$ and $\mu_\perp$ (in the region of metallic conductivity) on the distance between dislocations; $T = 4.2$ K.

$$\Delta\left(\frac{1}{H}\right)=\frac{e}{\pi c\hbar}\frac{1}{n}=\frac{4.85\cdot10^{6}}{n}, \tag{11}$$

where n is the carrier density. For our sample (Fig. 8, as well as Ref. 11) the oscillation period is $\Delta(1/H)=6.7\times10^{-6}$ Oe^{-1}; consequently the carrier density is

$$n=7.2\cdot10^{11}\,\text{cm}^{-2},$$

and is about one-tenth the heavy-hole density. Obviously, this value of n represents the light-hole density n_l.

Knowing the period of the oscillations and the intensity of the magnetic field corresponding to the intersection of the Fermi level with the given Landau level, we can determine the number N of this level. It follows from our data that $N=1$ at $H_1\approx100$ kOe and $N=2$ at $H_2\approx60$ kOe, whereas for the heavy holes these levels might be observed only in fields stronger by one order of magnitude. This confirms the dominant role of the light holes in the Shubnikov–de Haas effect.

As seen from relation (10), by measuring the Shubnikov–de Haas effect it is possible to determine the product mE_F from the period of the oscillations.

The oscillations were observed in samples with increased hole density and with the highest values of the mobility, $\mu=R\sigma\approx500$ cm^2/V-sec. It can therefore be assumed that in these samples the deformation near the intergrowth plane is smaller than in other samples, and the effective hole masses in the conducting layers can be close to their values in the volume. Assuming $m_l=0.042m_0$ as in the single-crystal, we find that the Fermi level in these samples lies approximately 40 meV lower than the top of the valence band. Obviously, the valence band is emptied up to this level and the levels for electron capture on the broken bonds lie above this energy.

In our measurements, Shubnikov–de Haas oscillations could be observed in germanium bicrystals only at the threshold of their possible appearance, i.e., under the condition

$$\omega_c\tau\approx1. \tag{12}$$

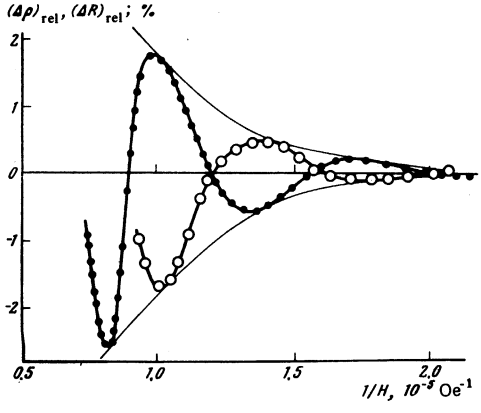

FIG. 8. Relative change of resistance and of the Hall coefficient in a magnetic field: ●—$(\Delta\rho)_{rel}=[\rho(H)-\bar{\rho}(H)]/\bar{\rho}(H)$, ○—$(\Delta R)_{rel}=[R(H)-\bar{R}(H)]/\bar{R}(H)$, where $\bar{\rho}(H)$ and $\bar{R}(H)$ are the average values of $\rho(H)$ and $R(H)$.

We can therefore use this relation to estimate the order of magnitude of the relaxation time τ. At $N=2$ the maximum deviation of ρ from the mean value is only a fraction of one per cent, and the corresponding magnetic field strength $H_2=60$ kOe can be regarded as the limit for relation (12). Then

$$\tau=3.7\cdot10^{-14}\,\text{sec}. \tag{13}$$

The value of τ for the two-dimensional case can also be estimated according to Ref. 12 from the relation

$$a\sim\frac{4(\omega\tau)^2}{1+(\omega\tau)^2}\exp\left(-\frac{\pi}{\omega\tau}\right), \tag{14}$$

where a is the deviation from the mean value at the extreme.

The measurements yield a ratio $a_1/a_2=3.5$; it follows then from (14) that $\tau\approx3.5\times10^{-14}$ sec. At these values of τ the light-hole mobility $\mu_l\approx1500$ cm^2/V-sec is approximately three times the heavy-hole mobility $\mu_h=490$ cm^2/V-sec. These data agree well with (7).

The smearing of the Landau levels can be estimated from the uncertainty relation. For light hole the level smearing is $\Delta E_l\approx\hbar/\tau_l=19$ meV, whereas the distance between the Landau levels at $H=100$ kOe is 28 meV. For the heavy holes the relaxation time can be estimated from the mobility $\mu_h=490$ cm^2/V-sec, which corresponds to $\tau_h\approx10^{-13}$ sec and a level smearing $\Delta E_h\sim\hbar/\tau_h=6$ meV, whereas the distance between the Landau levels at $H=100$ kOe is only 3 meV, thus confirming once more that under our conditions the oscillations connected with the heavy holes cannot be observed.

6. PHYSICAL PICTURE AND QUALITATIVE ESTIMATES

Germanium bicrystals with inclination angle $\theta\approx20°$ were investigated many times.[2] At low temperatures these bicrystals were investigated in Refs. 3 and 4. As already mentioned, our investigation was part of a search for high-temperature surface superconductivity. Although we could not observe it, our results may be of interest in the investigation of the electronic properties of layered structures.

As established in the first investigations[2,3] and confirmed by us, the electric conductivity of the layer adjacent to the intergrowth plane of a germanium bicrystal does not depend at helium temperatures on either the concentration or the type of electroactive impurity in the initial crystal. In our investigations the initial germanium single crystals were both of n-type and of p-type: the excess impurity density ranged from 4×10^{12} to 2×10^{16} cm^{-3}. The heat treatment of the bicrystals included heating in vacuum and in a melt of pure or doped lead (with Au, Ag, and Sn as impurities) at temperatures from 580 to 750 °C for 6–50 hours. In all cases, as follows from our measurement results, the crystal region directly adjacent to the cleavage plane has a rather high p-type conductivity down to temperatures obtainable by pumping off liquid helium.

The distribution of the potential along the crystal is similar to that cited in Ref. 3 and is shown in Fig. 9

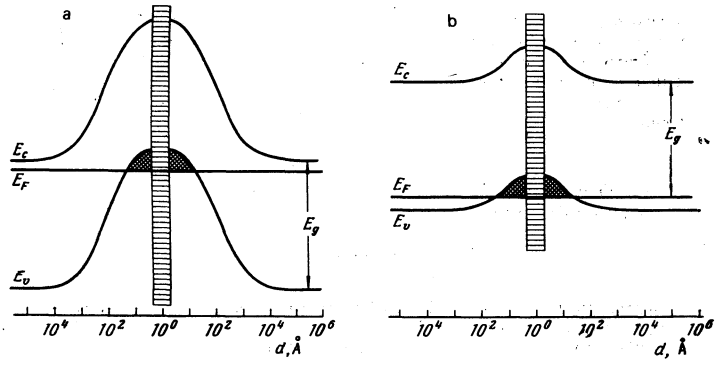

FIG. 9. Distribution of potential: a—in n-Ge in a direction perpendicular to the intergrowth plane of the bicrystal, b—in p-Ge. (The distance in angstroms is reckoned from the intergrowth surface. The region of the broken bonds is shaded. The free holes are cross-hatched. E_c and E_v are the edges of the conduction and valence bands; E_F—Fermi level, E_g-band gap.)

for n-Ge and p-Ge. The bending of the bands near the intergrowth plane ranges from several dozen millielectron volts in p-Ge to values exceeding the band gap $E_g \approx 0.7$ eV in n-Ge. Obviously, the decisive processes for the conducting layer are those occurring in the immediate vicinity of the intergrowth surface. The energy levels of the electrons at the unfilled valence bonds in the intergrowth plane are lower than in the interior of the crystal, and the electrons go over from the germanium atoms adjacent to the plane to the broken bonds in the dislocation, producing a negative charge on the cleavage plane and leaving holes in the valence band. With increasing surface charge, further transition of the electrons is hindered by the electric field, and an equilibrium state is established.

The surface density of the electrons on the broken bonds ranged in our case from 5×10^{12} to 1.8×10^{13} cm^{-2}. Since the number of broken bonds along each edge dislocation is of the order of 2×10^7 cm^{-1}, and the number of dislocations ranges from 2×10^6 to 1×10^7 cm^{-1}, their occupation coefficient is about 10%, and the average distance between captured electrons is 45 Å at $n=5\times10^{12}$ cm^{-2}. The electrons hardly take part in the electric conductivity, obviously because they are localized in sufficiently deep potential wells. The conductivty of the bicryatals is due to the motion of the free holes in a thin layer near the negatively charged plane.

Several approaches to an estimate of the thickness l of the hole layer at the cleavage plane are possible.

The Bohr radius of a hole moving around a localized electron is

$$r_B \approx \varkappa\hbar^2/m_h e^2 \approx 20\ \text{Å} \qquad (15)$$

in the three-dimensional case ($\varkappa$ is the dielectric constant).

The Debye radius can be estimated from the relation

$$r_D^2 = (\varkappa\hbar^2/4m_h e^2)\,(\pi/3N)^{1/3}. \qquad (16)$$

Assuming $\varkappa = 16$, $m_h = 0.36m_0$, and a volume concentrations $N = n/r_D$, we get $r_D \approx 15$ Å at $n = 5\times10^{12}$ cm^{-2}.

A tentative estimate of the conducting-layer thickness, obtained by Landwehr[13] in the Thomas-Fermi approximation, yields $\lambda = 24$ Å. All these estimates are highly approximate but yield close results.

In a thin layer adjacent to the intergrowth surface, at a thickness on the order of 20 Å, the number of impurity atoms are so small that they can be neglected in this case. This explains the independence of the properties of the conducting layer of the electric characteristics of the initial crystal.

When the distance d between the dislocations is appreciably less than 30 Å, the bicrystal conductivity is practically isotropic and is metallic, and more or less uniformly distributed in the conducting layer. When $d > 30$ Å the conducting layer is no longer homogeneous, the overlap of the wave functions decreases noticeably, and the conducting plane breaks up into strips with higher conductivity near the dislocation axes and much lower between them. With further increase of the distance between the dislocations, $d > 40$ Å, the conductivity along the dislocations also decreases sharply, apparently as a result of the increased isolation of the individual strips and the tendency of each of them to go over to conditions of one-dimensional conductivity. In this case both directions, along and across the dislocations, become practically nonconducting and the anisotropy coefficient is sharply decreased.

In a two dimensional region, in the case of degeneracy, the ratio of the heavy and light hole densities is equal to the ratio of their masses. In germanium, $m_h/m_l \approx 10$. On the other hand, a direct comparison of the data on the Hall and the Shubnikov–de Haas effects yields in our case $n_h/n_l \approx 20$. The possible cause of the discrepancy may be that the effective masses of the heavy and light holes become spontaneously equal to their values in the interior of the crystal. It is quite probable that the effective masses themselves and their ratio can be different near the intergrowth plane.

It can be assumed, however, as already mentioned, that the deformations play no significant role in samples with increased hole density, since the mobilities in them are quite high. Assuming that the ratio of the light and heavy hole effective masses in the layer are the same as in the interior of the crystals, the measurement results on the Hall and the Shubnikov–de Haas effects can be reconciled by assuming that the hole motion near the localized electrons takes places in two

thin layers adjacent to the negatively charged cleavage plane. The density n_h referred to one hole layer is then 7×10^{12} cm^{-2} and the ratio is $n_h/n_l = 10$, in accord with the ratio of the effective-mass ratio of the heavy and light holes in germanium.

[1]D. C. Tsui and S. J. Allen, Phys. Rev. Lett. **32**, 1200 (1974); C. J. Adkins, J. Phys. C **11**, 851 (1978).
[2]H. Matare, Defect Electronics in Semiconductors, New York, 1971.
[3]G. Landwehr and P. Handler, J. Phys. Chem. Solids **23**, 891 (1962).
[4]D. C. Licciardello and D. J. Thouless, Phys. Rev. Lett. **35**, 1475 (1975).
[5]B. M. Bul, N. V. Kotel'nikova, E. I. Zavaritskaya, and I. D. Voronova, Fiz. Tekh. Poluprovodn. **10**, 2277 (1976) [Sov. Phys. Semicond. **10**, 1351 (1976)].
[6]H. C. Montgomery, J. Appl. Phys. **42**, 2975 (1971).
[7]B. Lax, H. J. Zeiger, and R. N. Dexter, Physica (Utrecht) **20**, 818 (1954).
[8]R. Mansfield, Proc. Phys. Soc. London Sect. B **69**, 76 (1956).
[9]F. J. Blatt, Theory of mobility of electrons in solids, New York, 1957 [Russian Translation].
[10]T. Ando, Y. Matsumoto, and Y. Uemura, J. Phys. Soc. Jpn. **39**, 279 (1975).
[11]B. M. Bul and E. I. Zavaritskaya, Pis'ma Zh. Eksp. Teor. Fiz. **27**, 580 (1978) [JETP Lett. **27**, 547 (1978)].
[12]T. Ando and Y. Uemura, J. Phys. Soc. Jpn. **36**, 959 (1974).
[13]G. Landwehr, Phys. Status Solidi **3**, 440 (1963).

Translated by J. G. Adashko

Magnetic phase transitions in terbium orthoferrite

K. P. Belov, A. K. Zvezdin, and A. A. Mukhin

M. V. Lomonosov Moscow State University

(Submitted 7 September 1978)
Zh. Eksp. Teor. Fiz. **76**, 1100–1110 (March 1979)

Spin-reorientation transitions in $TbFeO_3$ are investigated. It is shown that they may be regarded as transitions of the Jahn-Teller type. The parameters of isotropic and of anisotropic R–Fe exchange are determined ($a \approx 70$ kOe, $b \approx 19$ kOe). It is shown that the R–Fe interaction shifts the antiferromagnetic ordering point of the Tb^{3+} ions and has a considerable effect on the cant angle of the magnetic sublattices of the Fe^{3+} ions (at $T \sim 5$ K, the change of the cant angle $\sim 40\%$). The importance is noted of the Van Vleck interaction of the quasidoublet ground state of the Tb^{3+} ion with the excited states.

PACS numbers: 75.30.Kz, 71.70.Ej, 75.50.Gg, 75.30.Et

1. INTRODUCTION

There have recently been intensive investigation of mangetic phase transitions of the spin-reorientation type (SR transitions) in rare-earth orthoferrites (ROF).[1] The variety of the magnetic properties observed in these compounds is determined, as a rule, by the peculiarities of the magnetism of the rare-earth ion (RI) in the orthoferrite structure and by the anisotropy of the exchange interaction of the rare-earth and iron ions. At low temperatures, the magnetic behavior of the RI depends substantially on the character of the wave functions of its lower energy levels. A good material for study of the influence of the ground state of the RI on the magnetic properties of a crystal is terbium orthoferrite, in which two phase transitions are observed at low temperatures; during them the weakly ferromagnetic moment, which at high temperatures is directed along the c axis of the crystal, with lowering of the temperature deviates to the a axis, and then again returns to its original state.[2]

In Refs. 3–5, phase transitions and H-T diagrams were investigated in $TbFeO_3$ at low temperatures, and the important role of dipole R-Fe interaction and of specimen shape in the phenomena considered was demonstrated. But in the theoretical investigation,[3-5] the nonisotropic part of the exchange R-Fe interaction was neglected, and this led to difficulties in the interpretation of the magnetic properties [in particular, of the $m_c(T)$ relation].

The present paper is devoted chiefly to explanation of the mechanisms of SR transitions in $TbFeO_3$ on the basis of microscopic ideas regarding the energy spectrum and the wave functions of the Tb^{3+} ion in $TbFeO_3$. It is shown that the high-temperature transition[1)] $\Gamma_4 - \Gamma_2$ can be regarded as a magnetic phase transition of Jahn-Teller type.[6] The low-temperature transition is more complicated. It occurs in two stages. First, at $T_N \approx 3.3$ K antiferromagnetic ordering occurs in the rare-earth subsystem ($\Gamma_2 \to \Gamma_{82}$); then at $T_{R2} \approx 3.1$ K this produces a reverse SR transition $\Gamma_2 - \Gamma_4$ in the subsystem of the Fe^{3+} ions, in which the RI go over to the purely antiferromagnetic configuration $\Gamma_8(A'_x G'_y)$.

During the comparison of the results of the theory with experiment, the R-Fe exchange-interaction constants are estimated.

2. Tb^{3+} IONS IN RARE-EARTH ORTHOFERRITES

In orthoferrites, the elementary cell contains four RI, which are located at crystallographic positions having local environmental symmetry C_s[2)]. The ground

0038-5646/79/030557-06$02.40